

The motional Stark effect diagnostic on TEXTOR-94: First measurements

T. Soetens^{a)}

*Department of Applied Physics, University of Ghent, Rozier 44, B-9000 Ghent, Belgium
ERM/KMS Laboratory for Plasma Physics, Brussels, Belgium*

R. Jaspers^{a)}

FOM-Institute for Plasma Physics, "Rijnhuizen," Nieuwegein, The Netherlands

E. Desoppere^{a)}

Department of Applied Physics, University of Ghent, Rozier 44, B-9000 Ghent, Belgium

(Presented on 10 June 1998)

We have developed a diagnostic to measure the motional Stark effect (MSE) on TEXTOR-94. This diagnostic allows us to measure locally the strength and direction of the magnetic field. Furthermore, the major radius of observation and the radial electric field are determined. Because the MSE diagnostic on TEXTOR-94 employs the full spectral information, in addition to the complete polarization, the measurements are independent from other experimental data. In this article we present the first preliminary results of the MSE diagnostic on TEXTOR-94. © 1999 American Institute of Physics. [S0034-6748(99)55701-8]

I. INTRODUCTION

To explain the confinement in tokamaks, knowledge of the electromagnetic configuration is indispensable, but measuring the internal electric and magnetic fields is not trivial.

Neutral beam spectroscopy has proven to be a successful means to measure the direction of the magnetic field in tokamak plasmas.¹⁻³ The fast beam atoms are subjected to the motional Stark effect, which arises when these atoms cross the magnetic field in the tokamak. On several machines this effect is exploited to determine the direction of the magnetic field. This is done using different methods such as dynamic polarimetry^{1,2} in TFTR and DIII-D or incomplete static polarimetry on JET.³ Recently, it has been shown that a motional Stark effect diagnostic can also successfully measure the radial electric field.^{4,5}

We have built a motional Stark effect diagnostic on TEXTOR-94. Our diagnostic uses complete static polarimetry as suggested by Voslamber.⁶ The advantage of this technique is that the complete polarization (i.e., the four independent Stokes parameters) and all the spectral information are available simultaneously. This diagnostic can determine locally the toroidal magnetic field, the poloidal magnetic field, and the radial electric field. These values are determined without using other measurements in the tokamak.

In the next section the motional Stark effect is explained in more detail. In Secs. III and IV the experimental setup and the first results are presented. Finally, these results are discussed in Sec. V.

II. MOTIONAL STARK EFFECT

The motional Stark effect arises from the electric field that the atoms in the fast neutral beam feel. Moving at high velocity in the magnetic field, the beam atoms are subjected to a Lorentz electric field:¹

$$\mathbf{E}_L = \mathbf{v}_B \times \mathbf{B}, \quad (1)$$

where \mathbf{v}_B is the beam velocity and \mathbf{B} the magnetic field.

A second field that contributes to the Stark effect is the radial electric field, which is necessary in a tokamak to balance the pressure gradient.⁴ However, this is a minor effect.

The electric field causes the Balmer α line of hydrogen (at $\lambda = 656.2$ nm) to split into equidistant components. As shown in Fig. 1 for each beam constituent there are 15 components, 9 of which have an observable intensity. The outer π components are polarized parallel to the electric field and the inner components have σ polarization in the plane perpendicular to the electric field. The polarization angle of the π components gives the direction of the Lorentz electric field and according to Eq. (1) the direction of the magnetic field.

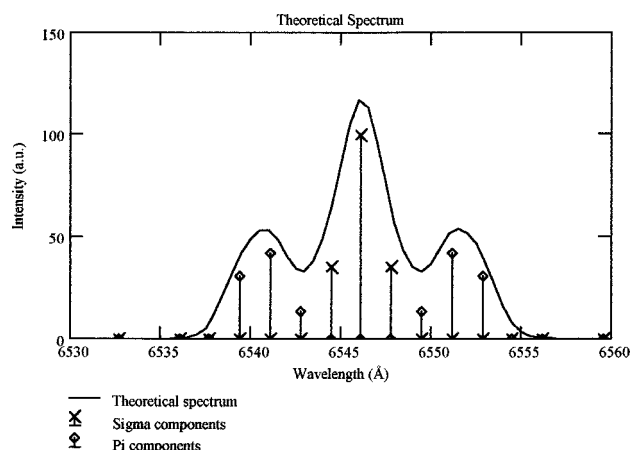


FIG. 1. Theoretical spectrum of the beam component of the Balmer α line. Nine of the 15 peaks are visible. The central peaks are σ polarized; the outer peaks are π polarized. The input parameters are: magnetic field 2.25 T, neutral beam acceleration voltage 46 kV, angle between line of sight and toroidal direction 10° , angle between neutral beam and toroidal direction 20° , and magnetic pitch angle 6° . The full line represents a convolution of Gaussians centered around the Stark peaks with an instrumental width.

^{a)}Partners in the Trilateral Euregio Cluster.

The spectral distance between the different components is proportional to the electric field strength and thus provides [Eq. (1)] the information about the magnitude of the magnetic field.

The main advantage of the motional Stark effect diagnostic compared to the HCN-laser polarimeter (another common diagnostic to measure the magnetic field direction, exploiting the Faraday rotation of a laser beam) is the localization of the measurements. The HCN-laser polarimeter performs line-integrated measurements and an Abel inversion of the results is necessary to obtain local information. Another advantage of our MSE polarimeter is that apart from the complete polarization, we measure all the spectral information. This allows simultaneous determination of the toroidal magnetic field, the poloidal magnetic field, the major radius, and thus the safety factor. Also the radial electric field can be calculated. Furthermore, knowledge of the complete polarization results in a self-calibration with respect to perturbations, such as a change of optical characteristics of in-vessel components as shown by Voslamber.⁶

The Doppler shift due to the motion of the fast beam atoms with respect to the stationary detector causes the beam emission spectrum to be completely separated from the plasma bulk spectrum. This Doppler shift depends on the angle θ between the line of sight and the neutral beam in the observation volume:

$$\frac{\Delta\lambda_D}{\lambda_0} = \frac{v}{c} \cos \theta, \quad (2)$$

with $\Delta\lambda_D$, λ_0 , v , and c are the Doppler shift, the unshifted wavelength of the H_α line, the beam velocity, and the speed of light, respectively. The angle θ and therefore the Doppler shift are indicators of the position of the observation volume in the plasma.

In normal plasma operation the radial electric field is very small and the relation between the magnetic pitch angle and the observed polarization angle is

$$\frac{1}{\tan \gamma_p} = \tan \gamma \sin \alpha + \frac{\cos \alpha}{\tan \Omega}. \quad (3)$$

The angles α , Ω , γ , and γ_p are the angle between the line of sight and the toroidal direction, the angle between the neutral beam and the toroidal direction, the magnetic pitch angle, and the measured polarization angle, respectively. This is illustrated in Fig. 2. When large density gradients or rotation velocities occur, a correction term has to be added⁴ as a consequence of the radial electric field of the plasma:

$$\frac{1}{\tan \gamma_p} = \tan \gamma \sin \alpha + \frac{\cos \alpha}{\tan \Omega} + \frac{\cos \alpha}{\sin \Omega \cos \gamma} \epsilon_R. \quad (4)$$

The quantity ϵ_R is a normalized radial electric field, defined as

$$\epsilon_R = \frac{E_R}{B v_B}. \quad (5)$$

Two parameters (γ and ϵ_R) have to be determined, so two polarization measurements have to be performed in each position. Since a hydrogen neutral beam normally consists of

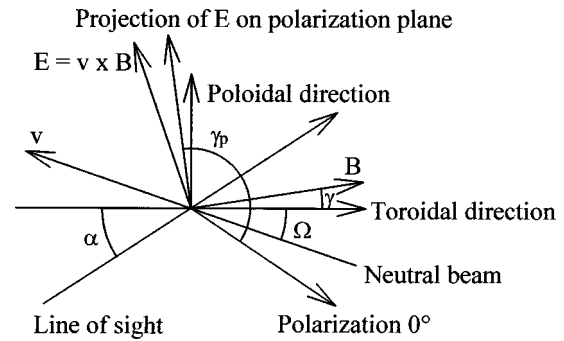


FIG. 2. Geometry of the observation volume of the motional Stark effect diagnostic. The polarization plane is perpendicular to the line of sight. The x axis lies in both the polarization plane and the toroidal-radial plane; the y axis is coincident with the poloidal direction. The angle γ_p is the measured polarization angle.

three energy constituents (normally labeled as full, half, and third energy components); in principle, three such measurements can be made on exactly the same position. On TEXTOR-94 we chose to use the full and half energy components of the spectrum emitted by the neutral beam atoms; the third energy component is measured as well and could be used to check the result.

Knowing the values of γ and ϵ_R we are able to calculate the magnitude of the magnetic field B from the spectral distance between two Stark peaks:

$$\Delta\lambda = \frac{3a_0 e \lambda_0^2}{2hc} B \sqrt{\sin^2 \Omega + (\cos \Omega \sin \gamma + \epsilon_R)^2}. \quad (6)$$

The quantities a_0 , e , and h are the Bohr radius, the electronic charge, and Planck's constant, respectively.

III. EXPERIMENTAL SETUP

TEXTOR-94 is a limiter tokamak with a circular cross section, a major radius of 175 cm, and a minor radius of 46 cm. The central magnetic field is normally 2.25 T. The heating systems are two ICRH antennas each of 2 MW and two neutral beam injectors each with a maximum accelerating voltage of 55 kV and a maximum injected power of 1.8 MW. The neutral beams are tangential, one co- and one counter-directed, and can operate with hydrogen, deuterium, helium-3, or helium-4.

The MSE diagnostic consists of a polarimeter and a spectrometer. The polarimeter has been constructed according to a scheme proposed by Voslamber.⁶ The purpose is to perform four independent measurements in the same position using different polarizations: polarization angles 0° , 45° , 90° , and circular polarization. The desired polarizations are acquired with two nonpolarizing plate beamsplitters, a polarizing cube beamsplitter, a polarizing filter tilted 45° , and a circular polarizer, arranged as in Fig. 3.⁷ The Stokes parameters, describing the full polarization of the emission, are traced from these intensities by a linear transformation. These measurements are done at four different positions in the plasma, all on the low field side in the range $R = [190-200]$ cm.

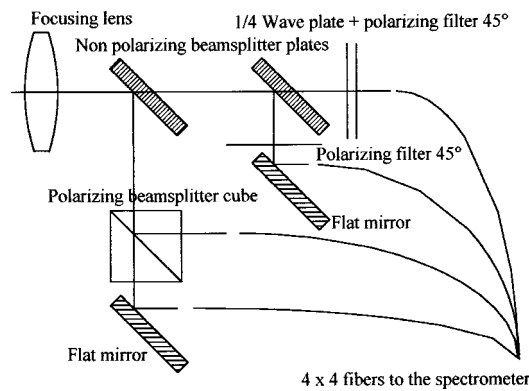


FIG. 3. Schema for the polarimeter construction. The emission is split into two equal beams by a plate beamsplitter, one of which is split into horizontal and vertical components by a cube beamsplitter. The other is split by the same type of plate beamsplitter. A polarizing film creates polarization tilted 45° and a circular polarizing filter the circular polarization.

The 4×4 signals are transported to a CCD-based Littrow spectrometer by quartz fibers. The spectrometer, optimized for the Balmer α line (6561 \AA), has an f number of $f/4.5$. The information recorded with the CCD camera can be read with a temporal resolution of 50 ms.

IV. FIRST RESULTS

The MSE diagnostic on TEXTOR-94 can only operate when the counter neutral beam injector is active. During TEXTOR shot 77312 there was a 1.18 MW hydrogen beam accelerated with 48.5 kV. A hydrogen beam has been chosen over a deuterium beam, because for testing purposes the larger Doppler shift was favorable. Other plasma parameters are: line-averaged electron density $3.1 \times 10^{19} \text{ m}^{-3}$, toroidal magnetic field 2.23 T and plasma current 359 kA.

Figure 4 shows the spectra recorded with the MSE diagnostic on TEXTOR-94. The optics have separated the σ and π polarized Stark peaks as expected. Two spectra have a lower intensity. This can be explained by the extra beamsplitter and the absorption of the polarizing film. We observe

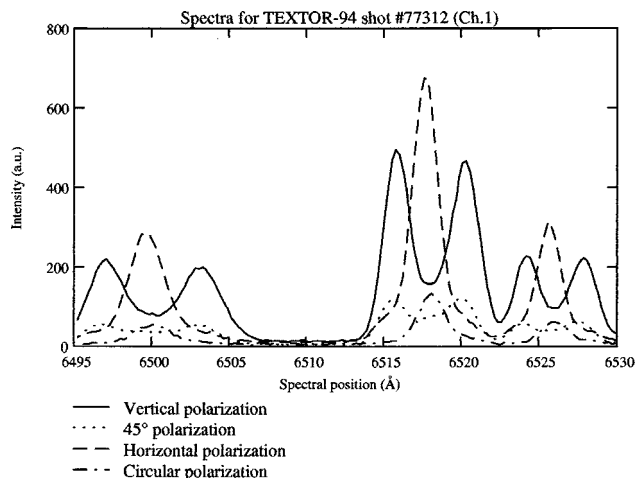


FIG. 4. Spectra recorded by the MSE diagnostic for TEXTOR-94 shot 77312, corresponding to channel 1. The polarizations are: horizontal, vertical, at 45° , and circular.

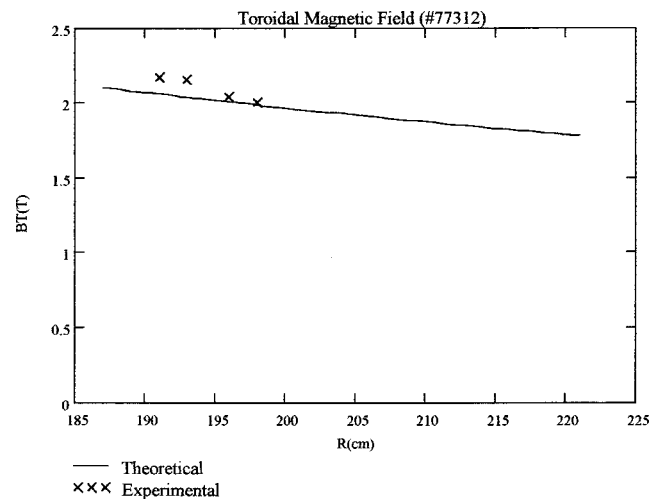


FIG. 5. Toroidal magnetic field profile for TEXTOR-94 shot 77312. Channel 1 gives the point on the low field side, channel 4 on the high field side. The position of the measured points is determined by the Doppler shift.

that the three beam components are well separated from the bulk plasma emission. The beam components are also separated from each other. Therefore, each of the beam components can be used to find the magnetic field and when they are coupled, a value of the radial electric field may be obtained as well.

The major radius of the observation volume is determined using two different methods. During a TEXTOR opening, an *in situ* measurement was done with an accuracy of 1–4 cm. The spot size of the focus in the plasma is 1 cm. The actual resolution however is somewhat larger, since the view is not completely tangential for the lines of sight looking towards the rather broad neutral beam [full width at half maximum (FWHM) of beam $\approx 20 \text{ cm}$]. The major radius is also determined during each measurement, making use of the Doppler shift. The statistical error during flat top state is smaller than 1 cm. The major radius determined during shots differs from the *in situ* measurement by less than 4%. The measurements for the observation positions during the shot will be used in the figures below, because in this latter method the effect of the beam width is incorporated.

In a tokamak, the toroidal magnetic field is inversely proportional to the major radius. Given the central toroidal magnetic field, mentioned previously, this results in the full line in Fig. 5. The measured points differ from this curve by less than 5%. The explanation for this difference can be found in a correction for the dispersion of the spectrometer or in paramagnetic or diamagnetic effects. This will be further investigated in the future.

The poloidal magnetic field is estimated theoretically by using the following form for the current density:

$$j(r) = j_0 \left[1 + q_a \left(\frac{r}{a} \right)^2 \right]^{-2}. \quad (7)$$

The quantities j_0 and q_a are the central current density and the safety factor at the edge of the plasma. The measured poloidal magnetic fields are of the same order of magnitude as those predicted by the theoretical curve (Fig. 6). Precise

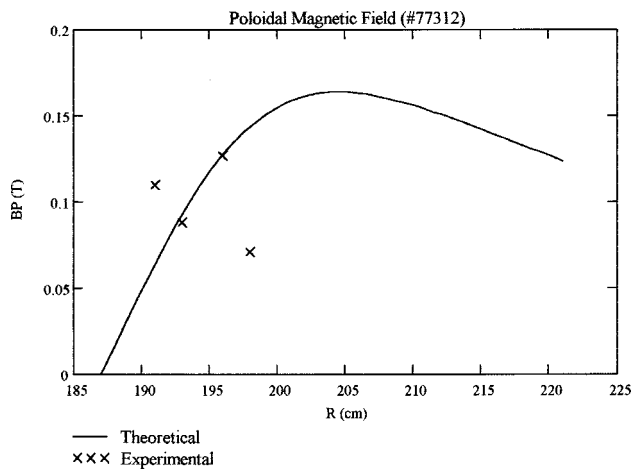


FIG. 6. Poloidal magnetic field profile for TEXTOR-94 shot 77312.

values were difficult to determine, because of the lack of an accurate calibration of the optical system. This calibration can only be done during an opening of the machine because the polarizing effect due to the reflection of the viewing port must be accounted for.

An attempt has been made to measure the radial electric field. The result was about 3×10^4 V/m. This value is less than 3% of the Lorentz electric field and thus a small perturbation. The radial electric field, given by

$$E_r = \frac{1}{Z_i e n_i} \nabla_r p_i - \nu_{pi} B_{Ti} + \nu_{Ti} B_{pi}, \quad (8)$$

can be estimated by the last term. A (measured) central rotation velocity of 100 km/s results in an estimated radial electric field of $1-2 \times 10^4$ V/m, which is of the same order as the inferred electric field. A better agreement was not anticipated because of the previously mentioned lack of calibration and the relative smallness of this radial electric field compared to the Lorentz field.

One of the more specific physical results was obtained in

the TEXTOR-94 radiation improved (RI) mode.⁸ The plasma edge is cooled by injecting neon gas, which dissipates energy by means of radiation. This results in an improved energy confinement. A first qualitative result of the MSE diagnostic is that the poloidal magnetic field rises in RI mode, showing a peaking of the current profile. This was confirmed by the results of the HCN-laser polarimeter.

V. DISCUSSION

We have built a motional Stark effect diagnostic on TEXTOR-94. This diagnostic measures the complete polarization of the spectral lines emitted by all three beam energy components. Our diagnostic uses complete static polarimetry.

First preliminary results show that the parameters R , B_T , B_P , and E_R can be determined to the right order of magnitude. However, the determination of precise values for especially B_P and E_R was hampered by the lack of reliable calibration factors. These calibration factors, necessary to trace the Stokes parameters, can only be obtained by an *in situ* calibration which will be performed in the near future. When the diagnostic is calibrated, a comparison between MSE results, laser polarimetry data, and theories can be started and the advantages of this diagnostic with respect to other methods can be tested.

¹D. Wróblewski, K. H. Burrell, L. L. Lao, P. Politzer, and W. P. West, *Rev. Sci. Instrum.* **61**, 3552 (1990).

²F. M. Levinton, S. H. Batha, M. Yamada, and M. C. Zarnstorff, *Phys. Fluids B* **5**, 2554 (1993).

³W. Mandl, R. C. Wolf, M. G. von Hellermann, and H. P. Summers, *Plasma Phys. Controlled Fusion* **35**, 1373 (1993).

⁴M. C. Zarnstorff, F. M. Levinton, S. H. Batha, and J. Synakowski, *Phys. Plasmas* **4**, 1097 (1996).

⁵B. W. Rice, K. H. Burrell, and L. L. Lao, *Nucl. Fusion* **347**, 517 (1997).

⁶D. Voslamber, *Rev. Sci. Instrum.* **66**, 2892 (1995).

⁷T. Soetens, R. Jaspers, and E. Desoppere, *Proceedings of the 18th Symposium on Plasma Physics and Technology*, edited by J. Pichal, Prague, June 17–20, 1997, pp. 36–38.

⁸A. M. Messiaen *et al.*, *Phys. Rev. Lett.* **77**, 2487 (1996).